

Journal of Photonics for Energy

SPIEDigitalLibrary.org/jpe

Functionalized pentacenes for dye-sensitized solar cells

Zhong Li
Karthik Shankar
Gopal K. Mor
Robert A. Grimminger
Chih-Min Lin
John E. Anthony
Craig A. Grimes

Functionalized pentacenes for dye-sensitized solar cells

Zhong Li,^a Karthik Shankar,^b Gopal K. Mor,^c Robert A. Grimminger,^d
Chih-Min Lin,^c John E. Anthony,^e and Craig A. Grimes^c

^aUniversity of Kentucky, Department of Chemistry, Lexington, Kentucky 40506

^bUniversity of Alberta, Department of Electrical & Computer Engineering, Edmonton, Alberta
T6G 2V4, Canada

^cPennsylvania State University, Department of Electrical Engineering and The Materials
Research Institute, University Park, Pennsylvania 16802

^dUniversity of Kentucky, Department of Chemistry, Lexington, Kentucky 40506

^eUniversity of Kentucky, Department of Chemistry, CP 125, Lexington, Kentucky 40506-0055
anthony@uky.edu

Abstract. Carboxylic acid functionalized pentacene-based dyes are synthesized and tested in dye-sensitized solar cells utilizing titania (rutile) nanowire arrays as the electron transporting photoanode. Functionalization on both chromophore and solubilizing substituents leads to materials demonstrating promising light-harvesting and energy-conversion properties in these large polycyclic aromatic compounds. © 2011 Society of Photo-Optical Instrumentation Engineers (SPIE). [DOI: [10.1117/1.3553781](https://doi.org/10.1117/1.3553781)]

Keywords: organic solar cells; organic dyes; titania; dye-sensitized solar cells.

Paper 10144SSPR received Aug. 15, 2010; revised manuscript received Jan. 2, 2011; accepted for publication Jan. 11, 2011; published online Mar. 10, 2011.

1 Introduction

The quest for low-cost photovoltaic devices has led to the utilization of organic materials in a variety of roles. Along with the rapid advances in bulk-heterojunction solar cells, which are slowly advancing toward 10% power-conversion efficiency (PCE),¹⁻³ dye-sensitized solar cells (DSSCs) are also a promising technology because of their low cost and relatively high efficiency. Introduced in 1991, initial DSSCs exhibited a 7% PCE,⁴ and quickly achieved ~10% with the development of new sensitizers.⁵ Despite these good efficiencies, disadvantages associated with rare-metal dyes and redox shuttle (I_3^-/I^-) carried by volatile organic solvent have slowed commercialization.^{6,7} To further improve DSSC performance, and potentially circumvent issues with metal-based dyes, all-organic sensitizers have been the focus of recent research efforts.⁸ Organic dyes are rapidly gaining in efficiency,⁹⁻¹⁸ approaching the PCE record (~11%) set by the current top performing rare-metal dye N719.¹⁹

Our group has developed a class of soluble pentacene derivatives with excellent hole mobility.^{20,21} With the eventual aim of developing materials for solid-state DSSCs,^{22,23} we endeavored to engineer a pentacene chromophore according to the general requirements for a dye to be used as a sensitizer in DSSCs. A functional sensitizer typically consists of a chromophore and an anchoring group, sometimes coupled by a conjugated linker (bridge). As the light-harvesting component, the chromophore is critical to device efficiency. Although the absorption breadth is not the only factor determining overall device performance, a general goal in sensitizer design is to cover as broad a spectrum as possible in the visible and near-IR region, where solar radiation at the planet surface is most intense. Most organic sensitizers absorb light below 600 nm while reasonably efficient near-IR/IR dyes used in DSSCs are only occasionally seen in literature.²⁴⁻²⁹ Pentacene chromophores, with potential absorption out to 750 nm,³⁰ could

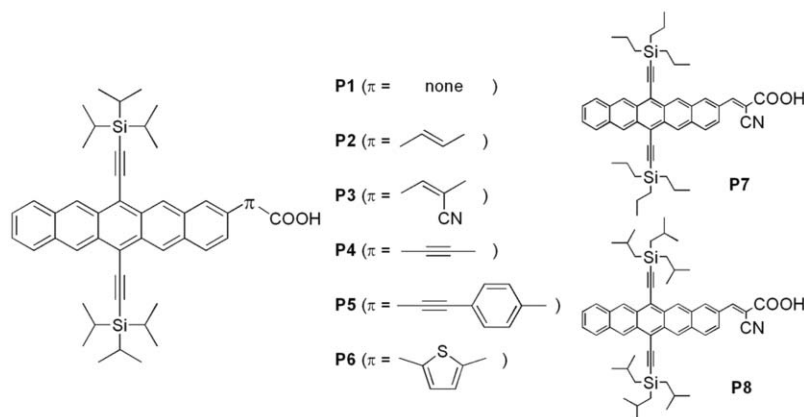


Fig. 1 Pentacene sensitizers P1–P8.

extend the window of performance for DSSCs, provided that there is efficient coupling between the acene and the inorganic matrix. We report here the synthesis of a series of pentacene dyes (Fig. 1) and the evaluation of their sensitizing efficiencies in liquid-junction DSSCs.

2 Experimental

Pentacene dyes P1–P6 were prepared as shown in Fig. 2. They feature solubilizing triisopropylsilylethynyl (TIPS) groups at the C-6 and C-13 positions and a –COOH anchoring group that is bridged by various conjugated linkers at the C-2 position. P7 and P8 share the core structure with P3, but the solubilizing trialkylsilylethynyl groups are engineered to enhance the solubility of resulting sensitizer.

2.1 Synthesis Details

As the simplest dye in this series, P1 has a –COOH group connected directly to the pentacene backbone. We were unable to prepare this compound by straightforward halide/CO₂ carboxylation of a 2-halopentacene in the presence of BuLi or Grignard reagent. Instead, a catalytic formylation³¹ of iodide 1 (Ref. 32) afforded aldehyde 2 in reasonable yield, which was followed by Ag₂O oxidation to acid P1. Dye P2 was obtained in two steps; a Heck reaction between 1 and *t*-butyl acrylate yielded ester 3, which was hydrolyzed to acrylic acid P2. Cyanoacrylic acid P3 was obtained by Knoevenagel condensation between aldehyde 2 and cyanoacetic acid. P7 and P8 were prepared in the same manner. Alkyne-linked dye P4 was prepared by hydrolysis of methyl ester 4, which was accessible by Sonogashira coupling between 1 and methyl propiolate. Dye P5 was also made by Sonogashira coupling using 4-ethynyl benzoic acid. Thiophene aldehyde 5 was obtained by Suzuki coupling of a thiophene carboxaldehyde in moderate yield and then oxidized to provide dye P6.

2.2 Device Fabrication

Vertically oriented TiO₂ nanowire arrays were synthesized by a hydrothermal method on fluorine doped tin oxide (FTO)-coated glass (TEC-8, 8 ohm/square) substrates. The substrates were initially cleaned by sonication in acetone, 2-propanol, and methanol, rinsed with deionized water, and dried in a nitrogen stream. These substrates were dipped in 0.1 M TiCl₄ solution for 8 h and then heated at 500°C for 1 h to obtain a layer of TiO₂ ~ 20 nm thick. To grow

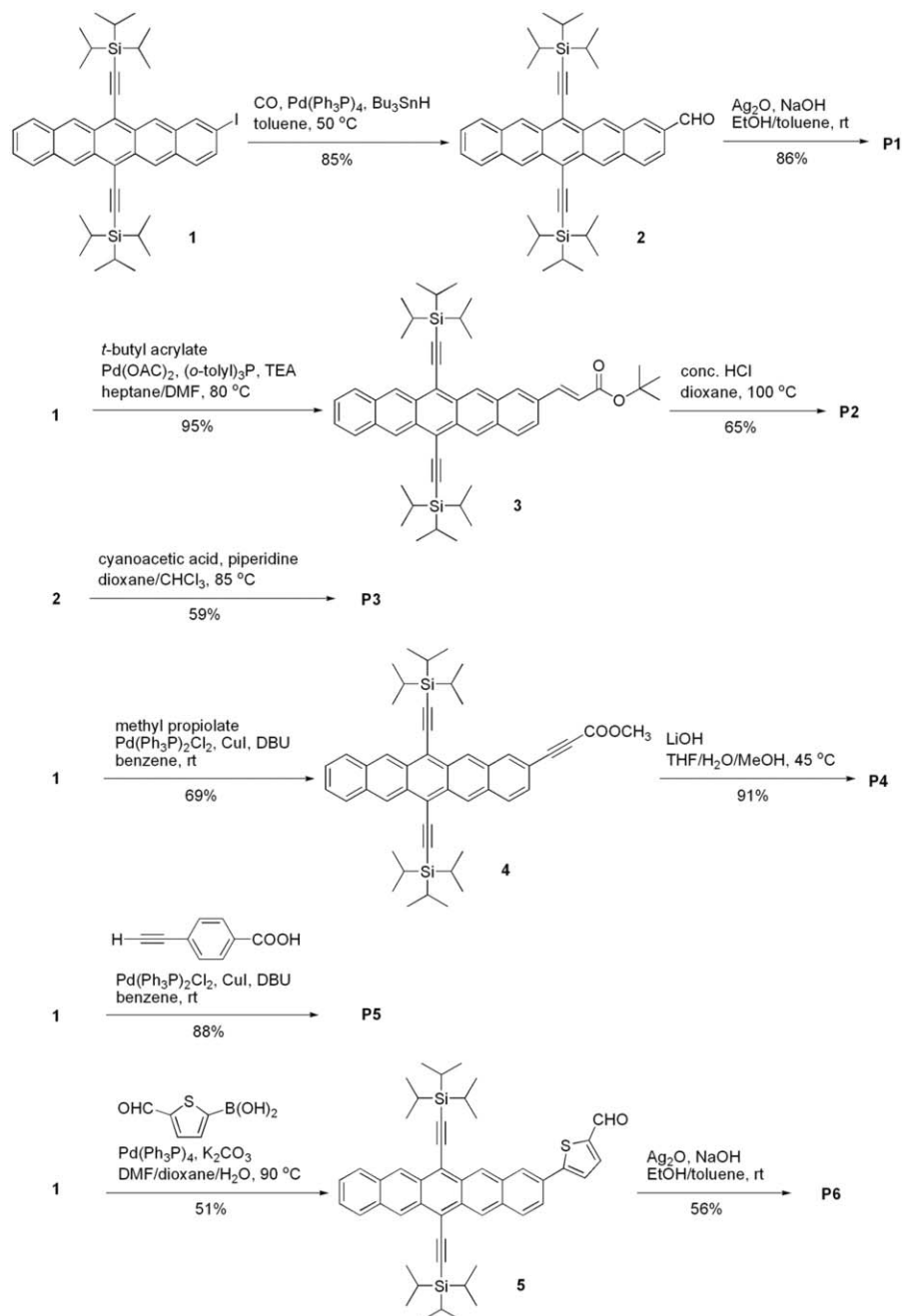


Fig. 2 Synthesis of P1-P6.

nanowire arrays, these treated FTO substrates were loaded into a sealed Teflon[®] reactor (23 ml volume) containing 10 ml of toluene, 1 ml of titanium tetrachloride (1 M in toluene), 1 ml of tetrabutyl titanate, and 1 ml of hydrochloric acid (37%). We conducted the growth of single-crystalline nanowires on transparent conducting oxide (TCO) solid substrate by a nonpolar solvent/hydrophilic solid interfacial reaction mechanism.³³ (A very different alkali hydrothermal growth process has also been used to synthesize single-crystalline rutile nanowire arrays.)³⁴ Because it is desirable to have a high surface area and close packing³⁵ of the nanowires for liquid solar cell applications, a high concentration of Ti⁴⁺ precursor was used. The reaction

took place at 160°C for 10 h. After the reaction was completed, the nanowire-covered FTO substrates were carefully washed with ethanol and annealed at 450°C for 30 min in air to remove the surface-adsorbed organic species. The nanowire arrays were $\sim 3.5 \mu\text{m}$ in length, 20 nm in width, and 5–10 nm in interwire spacing. All samples were further treated with oxygen plasma for 5 min at an RF power of 80 W to clean and hydroxylate the surface for better dye adhesion. The DSSCs were prepared using the following two procedures:

Method A: Nanowire array samples were coated with dye by immersion for 30–60 min in a 1-mM tetrahydrofuran (THF) solution of the respective pentacene dye (P1–P6). Liquid-junction solar cells were prepared by infiltrating the dye-coated TiO_2 electrode with redox electrolyte containing lithium iodide (0.1 M), iodine (0.01 M), tri-*n*-butyl phosphate (0.4 M), butyl methyl imidazodinium iodide (0.6 M), and guanidinium thiocyanate (0.1 M) in a mixture of acetonitrile and valeronitrile ($v/v = 15/1$). Conductive glass slides, sputter coated with 100 nm of Pt were used as the counter electrode. Electrode spacing between the nanowire and counter electrodes was ensured by using a 25- μm -thick SX-1170 spacer (Solaronix Inc., Aubonne, Switzerland). Photocurrent density and photovoltage were measured with active sample areas of 0.2 cm^2 using AM-1.5 simulated sunlight produced by a 500-W Oriel Solar Simulator, calibrated with a national renewable energy laboratory (NREL)-certified silicon solar cell.

Method B: Similar to method A except that nanowire array samples were coated with dye by immersion for 5 h in a 0.4-mg/mL toluene solution of the respective pentacene dye (P3, P7, and P8) at 70°C.

2.3 Computational Details

Density functional theory (DFT) calculations were performed in the Gaussian03 program package.³⁶ The geometries of P1–P6 were optimized at the B3LYP level using a 3–21G* basis set in vacuum using without any symmetry constraints. Electronic structure calculations were performed using a 6–31G* basis set. Molecular orbitals were visualized by GaussView 3.0 software.

3 Results and Discussion

P1–P6 were used to fabricate DSSCs but did not show impressive sensitizing results as their electronic characters indicate. Therefore, further molecular modifications and computational studies were applied to understand the possible reasons for their poor performance. Details will be presented in the following sections.

3.1 Solar Cell *I*–*V* Characterization

P1–P6 did act as effective sensitizers in DSSCs. Although their sensitizing capabilities seem to be limited, structure-property relationships are obvious. The linker that couples the pentacene chromophore and the anchor group plays a critical role in determining the sensitizing effect. The solubility of these dyes seems to be another important factor.

3.1.1 Linker effect

Initially, the solar cells were fabricated using method A. The subtle change in linker structure of sensitizers P1–P6 dramatically affects their performance in the devices (Fig. 3). Table 1 summarizes the key photovoltaic parameters for these materials. P1, which has no linker, shows the highest short-circuit current density ($J_{\text{SC}} = 1.49 \text{ mA/cm}^2$) as well as the highest open-circuit voltage ($V_{\text{OC}} = 0.6 \text{ V}$); however, its fill factor (FF) is only 0.38, the lowest in the group. In the case of P2 where a simple $-\text{C}=\text{C}-$ linker is introduced, comparable PCE ($\eta = 0.30\%$) is seen, although J_{SC} drops and FF rises. It is surprising to see a poor result from P3, which has an

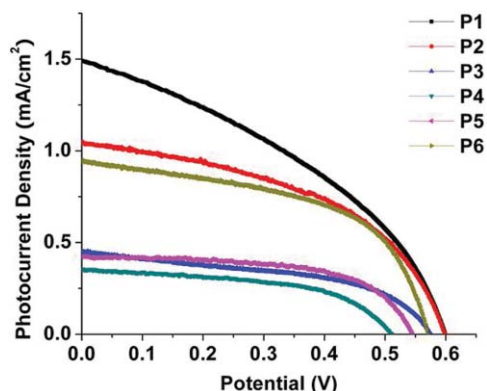


Fig. 3 J - V characteristics of DSSCs based on P1–P6.

extra cyano group on the vinyl linker. Incorporating cyanoacrylic acid is a well-known strategy in organic sensitizer development because the strong electron-withdrawing nature of $-\text{C}\equiv\text{N}$ has been demonstrated to facilitate the electron-injection process.³⁷ The unexpected low J_{SC} leads to overall poor performance by P3, indicating that a characteristic electronic property of the pentacene chromophore may mitigate the impact of the nitrile substituent. Switching to an alkyne linker (P4) results in the lowest PCE, arising from both poor J_{SC} and V_{OC} . This poor performance is also seen in alkyne-containing P5. Direct aryl attachment (P6), however, exhibits sensitizing ability similar to that observed in vinyl-linked P2, indicating that heteroacenes could serve as efficient electron donors to titania.

3.1.2 Dye solubility

The poor performance of P1–P6 arises mainly from low photocurrent, which indicates either low concentration of dye, poor light-harvesting abilities and/or inefficient electron injection. Dye loading of P1–P6 is less than ideal due to their poor solubility in the solvents most commonly used for DSSC loading, such as acetonitrile and methanol. These pentacene dyes are only sufficiently soluble in THF, which unfortunately destroys the polymer spacer specifying the active cell area. Therefore, the soaking time for the TiO_2 thin film in dye solution was limited, typically between 30 min and 1 h, which may result in an unsaturated concentration of sensitizer on the titania surface. To improve the solubility and enhance absorption, two more dyes were prepared, namely, P7 and P8. These two compounds have the same cyanoacrylic acid anchor as P3, while their greasier substituents, tri-*n*-propylsilylethynyl (TNPS) and tri-isobutylsilylethynyl (TIBS) respectively, provide them greater solubility. Indeed, in toluene the solubility of P3 at

Table 1 Photovoltaic parameters of DSSCs based on P1–P6.

Methods	Dye	V_{OC} (V)	J_{SC} (mA/cm^2)	ff	η (%)
A	P1	0.60	1.49	0.38	0.34
	P2	0.60	1.05	0.47	0.30
	P3	0.58	0.45	0.48	0.13
	P4	0.51	0.36	0.52	0.10
	P5	0.55	0.42	0.59	0.14
	P6	0.57	0.95	0.53	0.29
B	P3	0.59	1.02	0.52	0.31
	P7	0.61	1.69	0.49	0.50
	P8	0.58	1.74	0.47	0.47
	JK-2	0.77	7.79	0.56	3.34
	N719	0.76	6.57	0.66	3.30

room temperature is 0.3 mg/mL, while that of P7 and P8 is 0.5 and 0.4 mg/mL, respectively. It needs to be pointed out that it would make more sense to focus molecular optimization on P1, the top-performing dye in the series. However, different trialkylsilylethynyl groups have very different chemical tolerance toward conditions leading to P1-type chromophore, which made the TNPS and TIBS versions of P1 inaccessible.

The modification of trialkylsilyl groups should only optimize the staining process (method B) while leaving the sensitizing property unchanged due to the identical electronic structure of chromophore. Table 1 clearly demonstrates the solar cell performance (PCE) increased from 0.1 to 0.3% for P3 when the new fabrication method was used. Moreover, when the solubility of dye rises, PCE was enhanced even further, to 0.5% for P7 and 0.47% for P8. This improvement mainly results from a gain in J_{SC} , most likely due to the increase in concentration of chemisorbed dye afforded by the greater solubility.

It is worth noting that the low PCEs seen in our pentacene sensitizers also result from the device configuration: in these studies, particularly thin films of titania ($3.5 \mu\text{m}$) were employed, which limits the current produced by these dyes due to the short optical path. To have a meaningful comparison with traditional dyes, DSSCs based on N719 and organic dye JK-2¹⁸ were also tested under the same experimental conditions (Table 1). Their PCEs are about one-third of the best reported values,^{18,19} corresponding to the titania film thickness used in this study.

3.2 Absorption and Electrochemical Properties

As mentioned above, poor light-harvesting abilities and/or inefficient electron injection also can cause the relatively low performance of these pentacene dyes. The absorption spectra of P1–P6 solutions in THF [Fig. 4(a)] possess an intense $S_0 \rightarrow S_1$ band (ϵ is $\sim 10^4 \text{ M}^{-1} \text{ cm}^{-1}$) with fine vibronic progression in the near-IR region (between 550 and 700 nm). Figure 4(b) illustrates the absorption properties of these dyes chemisorbed onto the $3.5\text{-}\mu\text{m}$ nanocrystalline TiO_2 thin film.

There is no clear shift in the thin-film spectrum in comparison to the corresponding solution spectrum, indicating no obvious aggregation of dye molecules. For dyes whose photovoltaic performance in DSSCs is negatively impacted by aggregation, coadsorption of deoxycholic acid is often used to disrupt the aggregation and thus improve performance.^{38,39} However, TiO_2 nanowire array solar cells coated with a mixed monolayer of deoxycholic acid and P1–P6 were not found to exhibit any improved performance over the plain (P1–P6)–sensitized solar cells. This, together with the absence of clear shifts in the absorption data, rules out aggregation as the reason for low photocurrents. The broad absorptions extending well beyond 650 nm should yield good light harvesting for these materials.

The orbital energy levels were determined by a combination of differential pulse voltammetry (DPV) measurements and optical spectrum data (Table 2). The downhill energy offset by the LUMOs of P1–P6 ($> -3.50 \text{ eV}$ versus vacuum), relative to the conduction band edge (-4.00 eV versus vacuum) of TiO_2 , ensures sufficient thermodynamic driving force for electron injection. The uphill energy offset by the HOMOs ($< -5.00 \text{ eV}$ versus vacuum) with respect to that of iodide (-4.60 eV versus vacuum) supplies a desired negative Gibbs energy change for dye regeneration.⁴⁰ Computational results lead to the same conclusion on the favorable energy alignment of these pentacene sensitizers.

However, the incident photon to current efficiency (IPCE) of these sensitizers reach only 5% in the near-IR absorption window of pentacene chromophore. Examples using P1 and P3 are depicted in Fig. 4(c). Although the absorption properties and orbital energies of the pentacene sensitizers are acceptable, our results point to certain electronic properties of these pentacene dyes accounting for inefficient electron injection, leading to poor IPCEs and overall photocurrents.

In large conjugated systems, depending on their conformational and electronic structures, the electron-density distribution in the frontier orbitals can have a huge impact on molecular orbital mixing with the t_{2g}/e_g levels constituting the TiO_2 conduction band, as well as the geminate

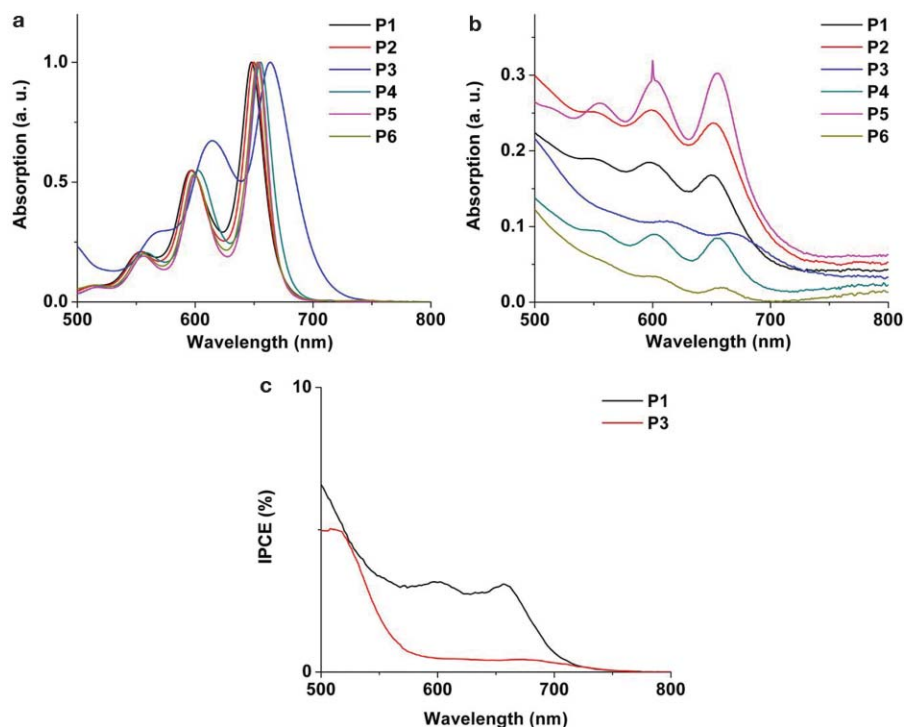


Fig. 4 (a) Normalized absorption spectra of P1–P6 in THF. (b) Absorption spectra of P1–P6 on TiO₂ films (systematically shift along the y-axis for clarity). (c) IPCE spectra of DSSCs sensitized with P1 and P3.

charge recombination between oxidized dye molecules and photoinjected electrons in TiO₂.⁴¹ Therefore, the relevant photophysical process will determine the output photocurrent.

As shown in Fig. 5, an ideal example of the electron-density distribution in the HOMO and LUMO of a sensitizer is shown by the high-performance organic dye JK-2 (calculation based on reported geometry).¹⁸ The excited-state orbital (LUMO) populates the anchor, facilitating significant mixing with the titania conduction band and, therefore, efficient electron injection. On the contrary, P3 clearly shows a less favorable pattern. It appears that the HOMO→LUMO excitation does not significantly redistribute the electron population from the pentacene core to the carboxylic acid anchor. Although the anchoring group gains a little electron population

Table 2 Experimental and computational energy levels of P1–P6.

Dye	λ_{\max} (nm)	$\epsilon_{\lambda \max}$ (M ⁻¹ cm ⁻¹)	E_{0-0}^a (eV)	E_{HOMO}^b (eV)	E_{LUMO}^c (eV)	E_{gap}^d (eV)	E_{HOMO}^d (eV)	E_{LUMO}^d (eV)
P1	648	2.26×10^4	1.75	-5.11	-3.36	1.87	-5.09	-3.22
P2	645	1.09×10^4	1.77	-5.05	-3.28	1.87	-5.10	-3.23
P3	664	1.50×10^4	1.64	-5.14	-3.50	1.78	-5.25	-3.46
P4	651	2.42×10^4	1.76	-5.16	-3.40	1.84	-5.15	-3.31
P5	651	2.66×10^4	1.77	-5.04	-3.27	1.84	-5.04	-3.20
P6	653	2.11×10^4	1.78	-4.97	-3.19	1.85	-5.05	-3.19

^a E_{0-0} values were estimated from the onset of solution absorption spectrum.

^b E_{HOMO} versus vacuum was measured by DPV under the following conditions: Pt working electrode and Pt counter electrode; supporting electrolyte, tetrabutylammonium hexafluorophosphate, 0.1 M solution in CH₂Cl₂, scan rate 20 mV/s. For ferrocene/ferrocenium (Fc/Fc⁺) in the same conditions, $E_{1/2} = -4.8$ V versus vacuum.

^c E_{LUMO} versus vacuum was estimated by $E_{\text{HOMO}} - E_{0-0}$.

^dCalculated.

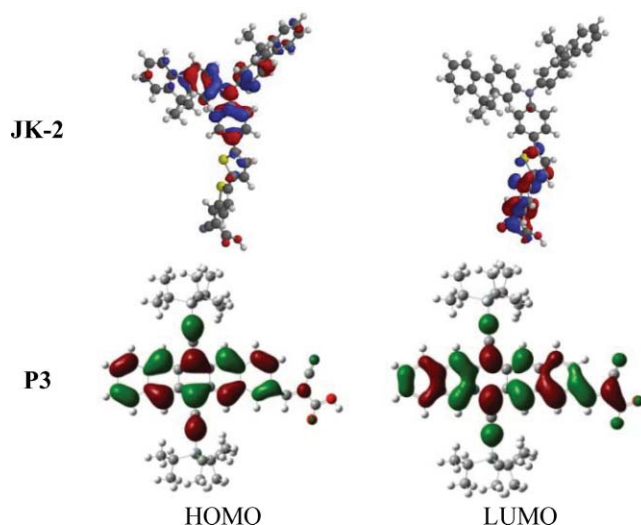


Fig. 5 HOMO/LUMO isodensity surface plots of JK-2 and P3.

in the LUMO, most of the orbital still extends over the entire molecule. As a result, there may be less orbital mixing potentially resulting in reduced photoexcited electron injection from sensitizer into TiO_2 . The pentacene core seems to hold delocalized electrons too strongly, even when a powerful electron-withdrawing group ($-\text{C}\equiv\text{N}$) is introduced. Similar situations were observed for all the other pentacene dyes reported here. Therefore, future work involving further molecular modification to provide a system with a better distinguished ground/excited states is necessary for a highly efficient pentacene-based sensitizer. The surprisingly high efficiency of the thiophene-substituted pentacene (P6) hints that heteroacenes, with their larger, more polarizable constituents, may be more amenable for use as dyes for DSSCs.

4 Conclusions

We have demonstrated the feasibility of using acene-based dyes for DSSCs. These large aromatics show promising light-absorption profiles and have appropriate orbital energies for use in DSSCs. Enhancements in solubility allow us to dramatically increase dye loadings and device performance, and the high hole mobility of this class of materials contributes to our ultimate goal of developing oligoacene-based solid state DSSCs. Further work based on acenes and heteroacenes, such as anthradithiophene, is currently ongoing and will be reported soon.

Acknowledgments

The authors thank the Department of Energy, Grant No. DE-FG36-08GO18074, for supporting this study.

References

1. L. Huo, J. Hou, S. Zhang, H.-Y. Chen, and Y. Yang, "A polybenzo[1,2-b:4,5-b']dithiophene derivative with deep HOMO level and its application in high-performance polymer solar cells," *Angew. Chem. Int. Ed.* **49**, 1500–1503 (2010).
2. Y. Y. Liang, D. Q. Feng, Y. Wu, S. T. Tsai, G. Li, C. Ray, and L. P. Yu, "Highly efficient solar cell polymers developed via fine-tuning of structural and electronic properties," *J. Am. Chem. Soc.* **131**, 7792–7799 (2009).
3. S. H. Park, A. Roy, S. Beaupre, S. Cho, N. Coates, J. S. Moon, D. Moses, M. Leclerc, K. Lee, and A. J. Heeger, "Bulk heterojunction solar cells with internal quantum efficiency approaching 100%," *Nat. Photon.* **3**, 297–295 (2009).

4. B. O'Regan and M. Grätzel, "A low-cost, high-efficiency solar cell based on dye-sensitized colloidal TiO₂ films," *Nature* **353**, 737–740 (1991).
5. M. K. Nazeeruddin, A. Kay, I. Rodicio, R. Humphry-Baker, E. Muller, P. Liska, N. Vlachopoulos, and M. Grätzel, "Conversion of light to electricity by cis-X₂bis(2,2'-bipyridyl-4,4'-dicarboxylate)ruthenium(II) charge-transfer sensitizers (X = Cl-, Br-, I-, CN-, and SCN-) on nanocrystalline titanium dioxide electrodes," *J. Am. Chem. Soc.* **115**, 6382–6390 (1993).
6. T. W. Hamann, R. A. Jensen, A. B. F. Martinson, H. Van Ryswyk, and J. T. Hupp, "Advancing beyond current generation dye-sensitized solar cells," *Energy Env. Sci.* **1**, 66–78 (2008).
7. S. Yanagida, Y. H. Yu, and K. Manseki, "Iodine/iodide-free dye-sensitized solar cells," *Acc. Chem. Res.* **42**, 1827–1838 (2009).
8. A. Mishra, M. K. R. Fischer, and P. Bauerle "Metal-free organic dyes for dye-sensitized solar cells: from structure: property relationships to design rules," *Angew. Chem. Int. Ed.* **48**, 2474–2499 (2009).
9. S. Hwang, J. H. Lee, C. Park, H. Lee, C. Kim, M. H. Lee, W. Lee, J. Park, K. Kim, and N. G. Park, "A highly efficient organic sensitizer for dye-sensitized solar cells," *Chem. Commun.* 4887–4889 (2007).
10. Z. S. Wang, Y. Cui, Y. Dan-Oh, C. Kasada, A. Shinpo, and K. Hara, "Thiophene-functionalized coumarin dye for efficient dye-sensitized solar cells: electron lifetime improved by coadsorption of deoxycholic acid," *J. Phys. Chem. C* **111**, 7224–7230 (2007).
11. H. Choi, C. Baik, S. O. Kang, J. Ko, M. S. Kang, M. K. Nazeeruddin, and M. Gratzel, "Highly efficient and thermally stable organic sensitizers for solvent-free dye-sensitized solar cells," *Angew. Chem. Int. Ed.* **47**, 327–330 (2008).
12. S. Ito, H. Miura, S. Uchida, M. Takata, K. Sumioka, P. Liska, P. Comte, P. Pechy, and M. Graetzel, "High-conversion-efficiency organic dye-sensitized solar cells with a novel indoline dye," *Chem. Commun.* **41**, 5194–5196 (2008).
13. H. Qin, S. Wenger, M. Xu, F. Gao, X. Jing, P. Wang, S. M. Zakeeruddin, and M. Gratzel, "An organic sensitizer with a fused dithienothiophene unit for efficient and stable dye-sensitized solar cells," *J. Am. Chem. Soc.* **130**, 9202–9203 (2008).
14. G. L. Zhang, H. Bala, Y. M. Cheng, D. Shi, X. J. Lv, Q. J. Yu, and P. Wang, "High efficiency and stable dye-sensitized solar cells with an organic chromophore featuring a binary π -conjugated spacer," *Chem. Commun.* 2198–2200 (2009).
15. R. Z. Li, J. Y. Liu, N. Cai, M. Zhang, and P. Wang, "Synchronously reduced surface states, charge recombination, and light absorption length for high-performance organic dye-sensitized solar cells," *J. Phys. Chem. B*, **114**, 4461–4464 (2010).
16. H. Im, S. Kim, C. Park, S. H. Jang, C. J. Kim, K. Kim, N. G. Park, and C. Kim, "High performance organic photosensitizers for dye-sensitized solar cells," *Chem. Commun.* **46**, 1335–1337 (2010).
17. W. D. Zeng, Y. M. Cao, Y. Bai, Y. H. Wang, Y. S. Shi, M. Zhang, F. F. Wang, C. Y. Pan, and P. Wang, "Efficient dye-sensitized solar cells with an organic photosensitizer featuring orderly conjugated ethylenedioxythiophene and dithienosilole blocks," *Chem. Mater.* **22**, 1915–1925 (2010).
18. S. Kim, J. K. Lee, S. O. Kang, J. Ko, J. H. Yum, S. Fantacci, F. De Angelis, D. Di Censo, M. K. Nazeeruddin, and M. Gratzel, "Molecular engineering of organic sensitizers for solar cell application," *J. Am. Chem. Soc.* **128**, 16701–16707 (2006).
19. M. K. Nazeeruddin, F. De Angelis, S. Fantacci, A. Selloni, G. Viscardi, P. Liska, S. Ito, B. Takeru, and M. G. Gratzel, "Combined experimental and DFT-TDDFT computational study of photoelectrochemical cell ruthenium sensitizers," *J. Am. Chem. Soc.* **127**, 16835–16847 (2005).
20. J. E. Anthony, J. S. Brooks, D. L. Eaton, and S. R. Parkin, "Functionalized pentacene: improved electronic properties from control of solid-state order," *J. Am. Chem. Soc.* **123**, 9482–9483 (2001).

21. M. M. Payne, S. R. Parkin, J. E. Anthony, C. C. Kuo, and T. N. Jackson, "Organic field-effect transistors from solution-deposited functionalized acenes with mobilities as high as $1 \text{ cm}^2 \text{ V}^{-1} \text{ s}^{-1}$," *J. Am. Chem. Soc.* **127**, 4986–4987 (2005).
22. U. Bach, D. Lupo, P. Comte, J. E. Moser, F. Weissortel, J. Salbeck, H. Spreitzer, and M. Gratzel, "Solid-state dye-sensitized mesoporous TiO_2 solar cells with high photon-to-electron conversion efficiencies," *Nature* **395**, 583–585 (1998).
23. J. H. Yum, P. Chen, M. Gratzel, and M. K. Nazeeruddin, "Recent developments in solid-state dye-sensitized solar cell," *ChemSusChem*, **1**, 699–707 (2008).
24. L. Beverina, R. Ruffo, C. M. Mari, G. A. Pagani, M. Sassi, F. De Angelis, S. Fantacci, J. H. Yum, M. Gratzel, and M. K. Nazeeruddin, "Panchromatic cross-substituted squaraines for dye-sensitized solar cell applications," *ChemSusChem* **2**, 621–624 (2009).
25. U. B. Cappel, M. H. Karlsson, N. G. Pschirer, F. Eickemeyer, J. Schoneboom, P. Erk, G. Boschloo, and A. Hagfeldt, "A broadly absorbing perylene dye for solid-state dye-sensitized solar cells," *J. Phys. Chem. C* **113**, 14595–14597 (2009).
26. T. Edvinsson, C. Li, N. Pschirer, J. Schoneboom, F. Eickemeyer, R. Sens, G. Boschloo, A. Herrmann, K. Mullen, and A. Hagfeldt, "Intramolecular charge-transfer tuning of perylenes: spectroscopic features and performance in dye-sensitized solar cells," *J. Phys. Chem. C* **111**, 15137–15140 (2007).
27. C. Li, Z. H. Liu, J. Schoneboom, F. Eickemeyer, N. G. Pschirer, P. Erk, A. Herrmann and K. Mullen, "Perylenes as sensitizers in hybrid solar cells: How molecular size influences performance," *J. Mater. Chem.* **19**, 5405–5415 (2009).
28. C. Li, J.-H. Yum, S.-J. Moon, A. Herrmann, F. Eickemeyer, N. G. Pschirer, P. Erk, J. Schoneboom, K. Mullen, M. Grätzel, and M. K. Nazeeruddin, "An improved perylene sensitizer for solar cell applications," *ChemSusChem* **1**, 615–618 (2008).
29. G. Zhou, N. Pschirer, J. C. Schoneboom, F. Eickemeyer, M. Baumgarten, and K. Mullen, "Ladder-type pentaphenylene dyes for dye-sensitized solar cells," *Chem. Mater.* **20**, 1808–1815 (2008).
30. S. S. Palayangoda, R. Mondal, B. K. Shah, and D. C. Neckers, "Synthesis of highly soluble and oxidatively stable Tetraceno[2,3-*b*]thiophenes and pentacenes," *J. Org. Chem.* **72**, 6584–6587 (2007).
31. V. P. Baillargeon and J. K. Stille, "Direct conversion of organic halides to aldehydes with carbon monoxide and tin hydride catalyzed by palladium," *J. Am. Chem. Soc.* **105**, 7175–7176 (1983).
32. Y. Shu, Y.-F. Lim, Z. Li, P. S. R., G. G. Malliaras, and J. E. Anthony, "A survey of electron-deficient pentacenes as acceptors in polymer bulk heterojunction solar cells," *Chem. Sci.* **2**, 363–368 (2011).
33. X. J. Feng, K. Shankar, O. K. Varghese, M. Paulose, T. J. Latempa, and C. A. Grimes, "Vertically aligned single crystal TiO_2 nanowire arrays grown directly on transparent conducting oxide coated glass: synthesis details and applications," *Nano Lett.* **8**, 3781–3786 (2008).
34. B. Liu, J. E. Boercker, and E. S. Aydil, "Oriented single crystalline titanium dioxide nanowires," *Nanotechnology* **19**, 505604 (2008).
35. K. Shankar, X. Feng and C. A. Grimes, "Enhanced harvesting of red photons in nanowire solar cells: evidence of resonance energy transfer," *ACS Nano* **3**, 788–794 (2009).
36. M. J. Frisch, *Gaussian 03*, rev. B.05, Gaussian, Inc., Wallingford (2004).
37. K. Hara, T. Sato, R. Katoh, A. Furube, Y. Ohga, A. Shinpo, S. Suga, K. Sayama, H. Sugihara, and H. Arakawa, "Molecular design of coumarin dyes for efficient dye-sensitized solar cells," *J. Phys. Chem. B* **107**, 597–606 (2003).
38. J. J. He, G. Benko, F. Korodi, T. Polivka, R. Lomoth, B. Akermark, L. C. Sun, A. Hagfeldt, and V. Sundstrom, "Modified phthalocyanines for efficient near-IR sensitization of nanostructured TiO_2 electrode," *J. Am. Chem. Soc.* **124**, 4922–4932 (2002).
39. A. Kay and M. Gratzel, "Artificial photosynthesis. 1. photosensitization of titania solar cells with chlorophyll derivatives and related natural porphyrins," *J. Phys. Chem.* **97**, 6272–6277 (1993).

40. A. Hagfeldt and M. Gratzel, "Light-induced redox reactions in nanocrystalline systems," *Chem. Rev.* **95**, 49–68 (1995).
41. W. R. Duncan and O. V. Prezhdo, "Theoretical studies of photoinduced electron transfer in dye-sensitized TiO₂," *Annu. Rev. Phys. Chem.* **58**, 143–184 (2007).

Zhong Li received his BS in polymer materials and engineering from Beijing Institute of Technology, China in 1999, and MS in polymer chemistry and physics from the Institute of Chemistry, Chinese Academy of Sciences in 2002. A year later, he moved to the State University of New York at Stony Brook to start his graduate study in organic chemistry and was awarded his PhD in 2008. He then joined professor John E. Anthony's lab at the University of Kentucky as a postdoc researcher. His research interests include the synthesis and applications of organic electronic materials, crystal engineering, and supramolecular chemistry.

Karthik Shankar obtained his BTech from the Indian Institute of Technology-Madras in 2000, and his MS and PhD in electrical engineering from The Pennsylvania State University in 2002 and 2007, respectively. Since August 2009, he has been an assistant professor in the Department of Electrical and Computer Engineering at the University of Alberta in Edmonton, Canada. His research interests are materials, phenomena, and devices at the intersection of nanotechnology and organic electronics. He is the author of 35 papers in refereed journals and has delivered numerous talks at major international conferences, such as the meetings of the Materials Research Society, SPIE, Device Research Conference, and Electronic Materials Conference.

Gopal K. Mor received his PhD in physics from Indian Institute of Technology Delhi, India, in 2002. He is presently working as research associate at the Materials Research Institute, at The Pennsylvania State University. His recent research interests are the design and fabrication of various excitonic solar cells, such as Förster resonance energy transfer (FRET)-type solid state solar cell, organic-inorganic-type ordered heterojunction solar cell, bulk heterojunction solar cell, and dye-sensitized solar cell. He also pursues research on water photoelectrolysis, hydrogen gas sensors, and the electrochemical anodic oxidation process of valve materials. He is the coauthor of the book *TiO₂ Nanotube Arrays: Synthesis, Properties and Applications*, Springer (2009).

Robert A. Grimminger received his BS in chemistry with a minor in physics from Juniata College in 2007. In the fall of that year, he began his dissertation work in the lab of Dennis J. Clouthier at the University of Kentucky, where he studies laser-induced fluorescence spectroscopy of transient species associated with semiconductor growth and interstellar processes. His interests include rotationally resolved spectroscopy, high-level quantum calculations, and small main group radicals.

Chih-Min Lin: biography not available.

John E. Anthony received his BA in chemistry from Reed College in 1989 and a PhD in chemistry from the University of California, Los Angeles, in 1994. His research interests include the development of new synthetic methodologies for fused aromatic compounds, and the design and synthesis of new organic semiconductors.

Craig A. Grimes received his BS in electrical engineering and BS in physics from the Pennsylvania State University in 1984, and his PhD in electrical and computer engineering from the University of Texas at Austin in 1990. His research interests include organic and inorganic heterojunction solar cells, photonic fuels, propagation and control of electromagnetic energy, and remote query environmental sensors. He has contributed ~300 archival journal publications, 12 book chapters, and 24 patents. Dr. Grimes is coauthor of *The Electromagnetic Origin of Quantum Theory and Light*; *The Encyclopedia of Sensors*; *Light, Water, Hydrogen: The Solar Generation of Hydrogen by Water Photoelectrolysis*; and *TiO₂ Nanotube Arrays: Synthesis, Properties and Applications*. Currently he is working on his latest book: *Electromagnetism and Quantum Theory: Quantum Jumps as Super-regenerative Transitions*.